Highly Active TiO_2N Photocatalysts Prepared by Treating TiO_2 Precursors in NH_3/Ethanol Fluid under Supercritical Conditions

Hexing Li,* Jingxia Li, and Yuning Huo

Department of Chemistry, Shanghai Normal University, 100 Guilin Road, Shanghai, China, 200234

Received: October 12, 2005; In Final Form: December 8, 2005

N-doped TiO_2 photocatalysts were prepared by pretreating the TiO_2 precursor in NH_3/ethanol fluid under supercritical conditions, denoted as TiO_2N(SC). In contrast to the TiO_2N(DC), obtained via direct calcination in which the N dopants were mainly present in the form of surface adsorbed NH_3 molecules, most N dopants in the TiO_2N(SC) were present in O−Ti−N and N−Ti−N nitrides, as confirmed by either the X-ray photoelectron spectroscopy (XPS) and or the Fourier transform infrared (FTIR) spectra. During liquid-phase oxidative degradation of phenol under irradiation with UV light characteristic of 365 nm, the TiO_2N(SC) exhibited much higher activity than either the TiO_2N(DC) or the TiO_2(SC), i.e., the undoped TiO_2 obtained under SCs. According to various characterizations including X-ray diffraction, transmission electron microscopy, FTIR, Brunauer−Emmett−Teller, XPS, and UV−vis diffuse reflectance spectra, the higher activity of the TiO_2N(SC) could be attributed to its higher surface area, larger pore volume, well-crystallized anatase, and stronger absorbance of light with longer wavelength. Meanwhile, the OH species resulted from the nitridation of TiO_2 could supply more HO• radicals, which were considered as powerful oxidants during phenol degradation. Furthermore, the electron-deficient nitrogen atoms in O−Ti−N nitrides could also account for the higher activity since it could inhibit the recombination between the photoinduced electrons and holes by capturing the photoinduced electrons. The activity of the TiO_2N(SC) first increased and then decreased with the increase of the N-content. The TiO_2N(SC)-1 with N/Ti molar ratio of 1.73% exhibited maximum activity, which was even much higher than P-25.

Introduction

Photocatalysis has been caused much attention owing to potential application in the environmental cleaning by mineralizing organic compounds and production H energy by decomposing water.[1−4] Among various photocatalysts, TiO_2 is most frequently employed owing to its cheapness, nontoxicity, and structural stability.[5−9] However, TiO_2 could be activated only by UV light due to its high energy band gap (ca. 3.2 eV for anatase), which seems a problem to make use of solar light since it contains only less than 5% UV light. Besides, the low quantum efficiency of the TiO_2 also limited its application. Great attempts have been made to improve the catalytic performance of the TiO_2 photocatalyst.[1,4,10] Among various dopants, the modification of TiO_2 with the N dopant seems a powerful way to extend the adsorption light from UV to visible area, since the substitution of the lattice oxygen with nitrogen might narrow the band gap by mixing the N_{1S} and O_{1S} states.[11−13] Up to now, almost all N-doped TiO_2 samples were prepared by treating TiO_2 under NH_3 atmosphere at very high temperature. Besides the energy waste, the treatment at high temperature usually resulted in the low surface area due to agglomeration and collapse of pore structure. Furthermore, mixed crystalline phases of anatase and rutile may usually be formed at high temperature. As is well known, treatment of catalyst precursor under supercritical conditions (SCs) may maintain the pore structure as that in the gel owing to the absence of surface tension.[14−17] In our previous papers, we reported the preparation of both the TiO_2 and the SO_4^{2-}-doped TiO_2 under SCs.[18,19] Besides the high surface area, large pore size, and high crystallization degree of anatase, it was also found that nearly all SO_4^{2-} dopants embedded in the TiO_2 network while only trace of SO_4^{2-} dopants were left on the surface via chemisorption. In this paper, we reported a new N-doped TiO_2 photocatalyst prepared by treating TiO_2 precursor with NH_3/ethanol fluid under SCs, which exhibited higher activity than either the undoped TiO_2 or the N-doped TiO_2 obtained via direct calcinations (DC). On the basis of various characterizations, the promoting effects on the activity of both the N modification and the supercritical treatment were discussed briefly.

Experimental Section

A. Catalyst Preparation. At 313 K, 10 mL of $Ti(On\text{-}C_4H_9)_4$ was added slowly into 40 mL of ethanol to form solution A. Meanwhile, 2.5 mL of dilute HNO_3 solution (1:5, v/v) was mixed with 10 mL of ethanol to prepare solution B. Then, the solution B was added dropwise into the solution A within 20 min under vigorous stirring. The solution was stirred continuously for 1.0 h until the formation of TiO_2 gel. After being aged for 48 h at 318 K, the as-prepared TiO_2 xerogel was transferred into 500 mL of autoclave with 250 mL of ethanol solution containing the desired amount of NH_3. After being swept by pure N_2 for 15 min to remove the O_2 inside, the autoclave was heated at the speed of 4 K/min up to 533 K, during which the pressure reached gradually to 13 MPa. The system was kept under such SCs for 2 h and then the vapor was released slowly, and then was allowed to cool slowly down to room temperature in the N_2 flow. The obtained yellow solid was further calcinated at high temperature for 8 h to remove the residual organic compounds resulted from the hydrolysis of the $Ti(On\text{-}C_4H_9)_4$

* To whom correspondence should be addressed. E-mail address: HeXing-Li@shnu.edu.cn. Fax: +86-21 64322272.

10.1021/jp055830j CCC: $33.50
Published on Web 01/07/2006

and the solvent. A preliminary test demonstrated that the optimum calcination temperature was 573 K. Finally, the as-prepared sample was crushed and kept in a vacuum until the time of use. These samples were denoted as TiO_2N(SC), where SC refers to SCs. The nitrogen content in the TiO_2N(SC) could be easily adjusted by changing the concentration of NH_3 in ethanol solution and was denoted as TiO_2N(SC)-X, where X = 1, 2, 3, 4, corresponding to NH_3 concentrations of 0.6, 1.2, 2.4, and 3.6 M. For comparison, the corresponding N-doped TiO_2 samples were also prepared by stirring the TiO_2 precursor for 6 h in 250 mL solution containing different amount of ammonia, followed by DC at 573 K. These samples were represented as TiO_2N(DC)-X.

B. Catalyst Characterization. The structure of the as-prepared samples was determined by both X-ray diffraction (XRD, Rigacu Dmax-3C, Cu Kα radiation) and Fourier transform infrared (FTIR) (NEXUS 470). Their light absorption abilities were analyzed by UV−vis diffuse reflectance spectra (DRS, MC-2530). The N_2 adsorption−desorption isotherms were determined by the Brunauer−Emmett−Teller (BET) method (NOVA 4000) at 77 K, from which the surface area (S_{BET}), pore volume (V_P), and average pore diameter (d_P) were calculated by using the BJH method. Both the surface morphology and the particle size were observed through transmission electronic micrography (TEM, JEM-2010). The surface electronic states were analyzed by X-ray photoelectron spectroscopy (XPS, Perkin-Elmer PHI 5000C). The molar ratio of N/Ti in the TiO_2N samples was determined by using 0.477 and 2.001 as the PHI sensitivity factors to N_{1S} and $Ti2P_{3/2}$, respectively, offered by Perkin-Elmer Company.

C. Activity Test. The liquid-phase photocatalytic degradation of phenol was carried out at 303 K in a self-designed 200-mL glassy reactor containing 0.05 g of catalyst and 30 mL of 0.05 g/L phenol aqueous solution. The reaction system was exposed in the air, and the photocatalytic oxidation was initiated by irradiating the reactor with three 6-W lamps (located at 4 cm above the solution) with the characteristic wavelength of 365 nm. To ascertain the role of mass transfer, the catalyst amount was varied from 0.02 to 0.10 g and the speed of agitation was varied from 800 to 1200 rpm. In view of the observation that the reaction rate was independent of the stirring rate and that it varied linearly with the catalyst amount, it could be concluded that the stirring rate of 1000 rpm was high enough so that the phenol degradation rates were independent of mass transfer. The reaction mixture was sampled every hour, and the phenol left in the solution was analyzed by a UV spectrophotometer (UV 7504/PC) at the characteristic wavelength of phenol (λ = 270 nm), from which the phenol degradation yield, i.e., the phenol conversion (%) was calculated. Preliminary tests showed that there was a good linear relationship between the absorbance and the phenol concentration. Meanwhile, experimental results also confirmed that only less than 3% phenol decomposed after reaction for 4 h in the same conditions in the absence of either the photocatalyst or the UV light and, thus, could be neglected in comparison with that in the presence of both the catalyst and the UV source. The reproducibility of the results was checked by repeating the results at least three times and was found to be within acceptable limits (±5%).

Results and Discussion

Figures 1 and 2 are the FTIR spectra of the TiO_2 and TiO_2N samples obtained via DC or through the pretreatment under SC. One could see that, besides the absorption peak at 1630 cm^{-1} belonging to the Ti−O structure, the TiO_2N(DC) exhibited only one additional peak at 1390 cm^{-1} corresponding to the surface adsorbed NH_3 molecules.[20] Although the absorption peak indicative of surface-adsorbed NH_3 was also observed, the TiO_2N(SC) displayed five new absorbance peaks. The peaks 1450, 1220, and 1160 cm^{-1} could be attributed to the nitrogen atoms embedded in the TiO_2 network,[20,21] while the absorption peaks at 3400 and 2850 cm^{-1} were assigned to the OH species.[22] These results clearly demonstrated that the treatment of the TiO_2 precursor in ammonia solution under SCs resulted in not only the chemisorption of NH_3 molecules on the TiO_2 surface but also the nitridation of the TiO_2 in network. Scheme 1 briefly

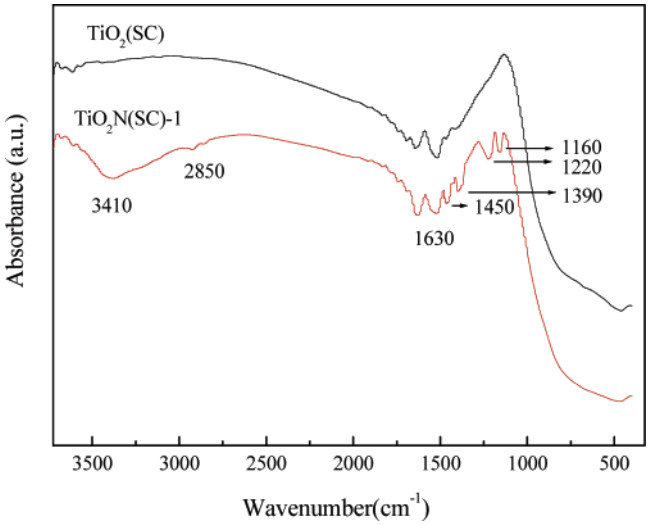

Figure 1. FTIR spectra of the TiO_2(SC) and TiO_2N(SC) samples.

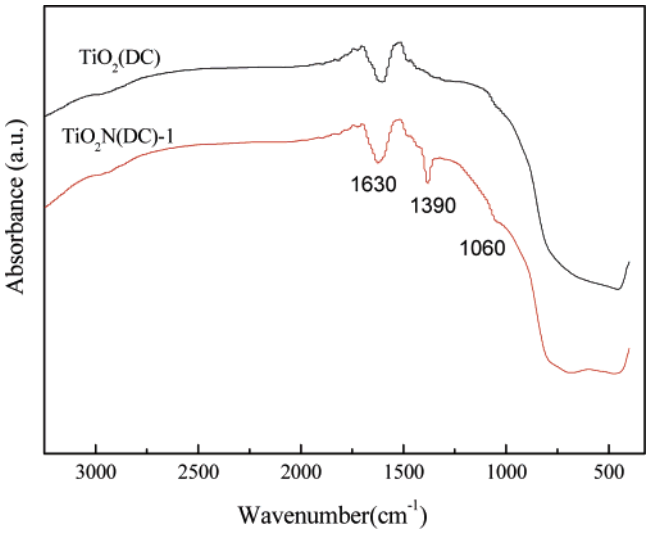

Figure 2. FTIR spectra of the TiO_2(DC) and TiO_2N(DC) samples.

SCHEME 1: Formation of O−Ti−N and N−Ti−N Nitrides

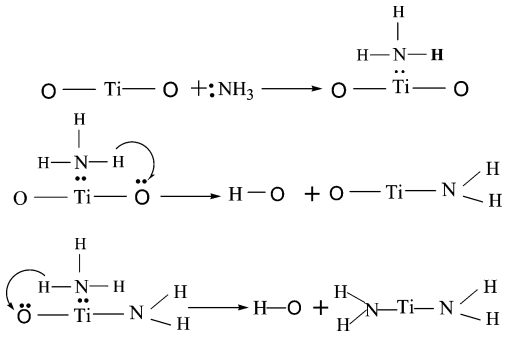

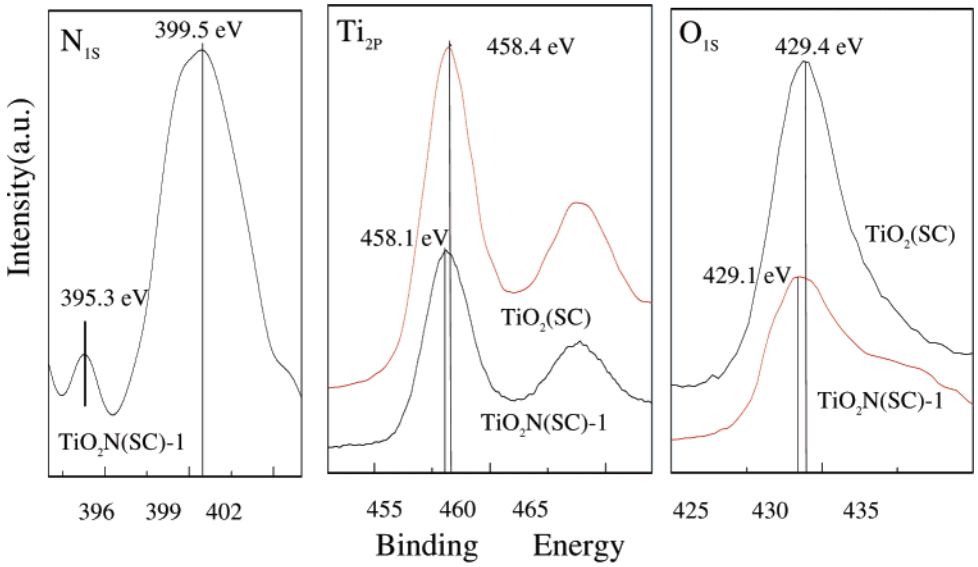

Figure 3. XPS spectra of the TiO_2(SC) and TiO_2N(SC) samples.

described the nitridation process. Step 1 is the surface adsorption of NH_3 molecules. The nitridation occurred in steps 2 and 3 by replacing the oxygen atom in the TiO_2 with the nitrogen atom in the NH_3, resulting in the formation of the O−Ti−N and the N−Ti−N as well the OH species.[23]

The Scheme 1 could be further confirmed by the XPS characterization. As shown in Figure 3, two kinds of N species were detected in the N_{1S} level. Most N species in the TiO_2N(SC) existed in the nitrides, corresponding to the binding energy (BE) of 399.5 eV, while only trace N species were present in the form of surface adsorbed NH_3 molecules, with the BE located at 395.3 eV. In comparison with the pure TiN,[24] the BE of nitrogen in the nitrides positively shifted by 0.30 eV. From the Ti_{2P} and O_{1S} levels, one could also find that the peaks corresponding to either the Ti or the O in the TiO_2N(SC) shifted negatively by 0.3 eV in comparison with the pure TiO_2(SC). These results further confirmed the formation of the O−Ti−N, in which partial electrons transferred from the N to the Ti and the O due to the higher electronegativity of oxygen than that of nitrogen, making N electron deficient while both the Ti and O were electron enriched, as shown in the following diagram

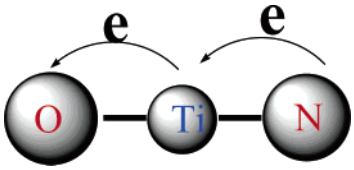

From the relative areas of the XPS peaks corresponding to $Ti2P_{3/2}$ and N_{1S}, the N/Ti molar ratios ($X_{N/Ti}$) in the form of nitrides of the TiO_2N(SC) samples were calculated by using 0.477 and 2.001 as the PHI sensitivity factors to N_{1S} and $Ti2P_{3/2}$, respectively. The $X_{N/Ti}$ in the TiO_2N(SC)-1 was determined as 1.73%, indicating that only a very little amount of NH_3 in the NH_3/ethanol fluid could be embedded in the TiO_2 network by nitridation. The $X_{N/Ti}$ increased from 1.73 to 2.0% when the NH_3 concentration in the ethanol fluid used in the SCs increased from 0.6 to 3.6 M, showing that the NH_3 concentration in the ethanol fluid had only little influence on the $X_{N/Ti}$. However, considerable increase of the surface adsorbed NH_3 molecules was observed.

The XRD patterns demonstrated that all the TiO_2 and TiO_2N samples were present in the anatase phase regarless of the

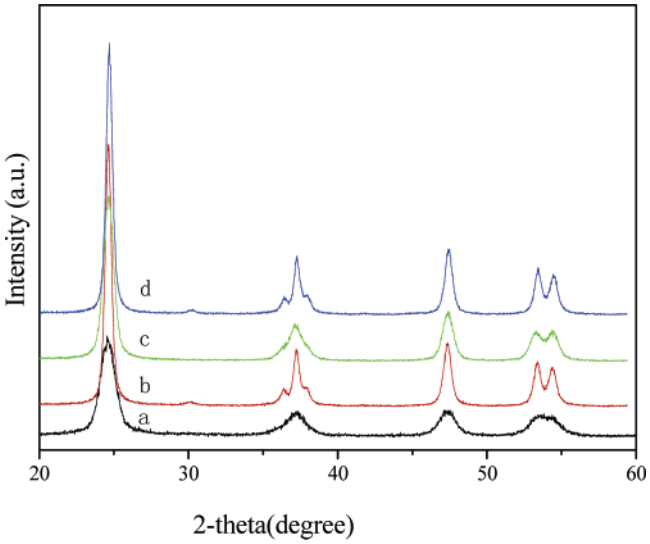

Figure 4. XRD patterns of (a) TiO_2(DC), (b) TiO_2N(DC), (c) TiO_2(SC), and (d) TiO_2N(SC).

pretreatment methods (DC and SC), as shown in Figure 4. The broad peaks observed in the TiO_2(DC) implied the poor crystallization degree of anatase. Either the N-doping or the pretreatment under SCs could enhance the crystallization degree of the anatase phase. Thus, modification of the TiO_2 under SCs resulted in the best-crystallized anatase. Figure 5 shows the XRD patterns of the TiO_2N(SC) calcinated at elevated temperatures from 773 to 1173 K. In comparison with that of the TiO_2N(SC) calcinated at 573 K, no significant changes were observed even after being calcinated at 1173 K. This again supported the above conclusion that the TiO_2N(SC) already reached well crystallization degree of anatase even after calcination at low temperature (573 K), and in turn, increase the calcination temperature did not show significant improvement on the crystallization degree. Furthermore, no rutile phase corresponding to 2θ around 32.0° was found in the TiO_2N(SC) even after being calcinated at 1173 K. Taking into account that the transformation from anatase to rutile occurred at 673 K for the TiO_2(DC) and at 973 K for the TiO_2(SC), respectively,[18,19] it was obvious that modification with nitrogen under SCs could greatly enhance the thermal stability of the TiO_2 photocatalyst.

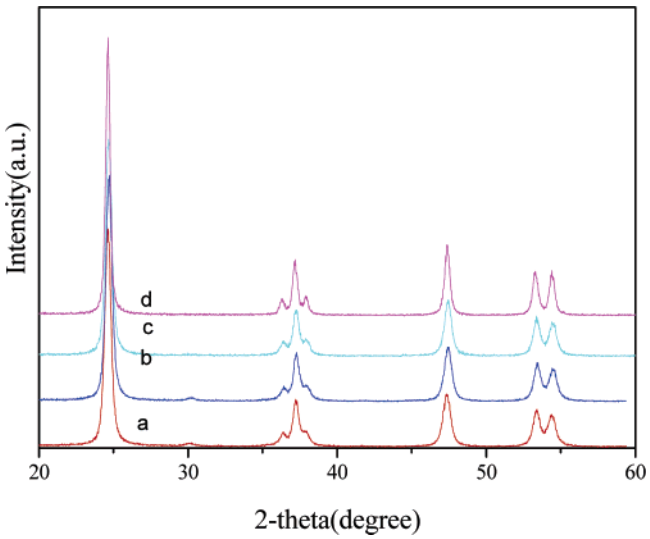

Figure 5. XRD patterns of the TiO_2N(SC) sample after being calcinated at (a) 573 K, (b) 973 K, (c) 1073 K, and (d) 1173 K.

Figure 6 shows the TEM morphology of different samples. The TiO_2(DC) was present in the form of spherical particles with the average size around 10−15 nm, while both the TiO_2(SC) and TiO_2N(SC) were present in cubic particles. The particle size increased in the order of TiO_2(DC), TiO_2(SC), and TiO_2N(SC). According to the above XRD characterizations, the TiO_2(DC) was present in poor crystallization degree, corresponding to the smaller size and spherical shape of the TiO_2(DC) particles. The pretreatment of the TiO_2 precursor under SCs favored the crystallization of anatase and growth of crystallites,[14] which could sufficiently account for the increase of particle size and the change of particle morphology from spherical to cubic shape, taking into account that the anatase crystal was comprised of cubic cells, as shown in Figure 7. The N modification could further improve the crystallization process of anatase and the growth of the crystallites, and thus the particle size of the TiO_2N(SC) was slightly bigger than that of the undoped TiO_2(SC). Though the particle size increased, the pretreatment under SCs could effectively inhibit the particle agglomeration,[15] more homogeneous distribution of either the TiO_2(SC) or the TiO_2N(SC) than that of the TiO_2(DC) was observed, as shown in Figure 6.

Table 1 listed some structural parameters of the as-prepared samples. First, the TiO_2(SC) exhibited much higher a S_{BET} value than the corresponding TiO_2(DC), which could be mainly attributed to the increase of pore volume (V_P) since the TEM morphologies demonstrated that the TiO_2(SC) exhibited bigger particle size than the TiO_2(DC). This could be easily understood by considering the unique role of the SCs since removal of the solvent under such conditions might maintain the pore structure in the gel owing to the lack of surface tension effect .[14,15,20] However, severe collapse of the pore structure would occur when the solvent in the gel was removed by direct drying, resulting in an abrupt decrease in the pore volume and, thus, the surface area. Meanwhile, the homogeneous distribution of TiO_2 nanoparticles, i.e., the less particle agglomeration, could also account for the higher S_{BET} of the TiO_2(SC). Secondary, with the increase of NH_3 concentration in the ethanol fluid used for supercritical treatment, both the S_{BET} and the V_P of the TiO_2(SC) increased gradually while the pore size (d_P) remained almost constant. One possible reason was the increase of the surface O−H and N−H species, as discovered by Brodsky et al.[25] Meanwhile, the addition of NH_3 in the ethanol fluid used in SCs tended to stabilize gel pore structure or colloidal particles via hydrogen bonding and steric effects[26] and could inhibit the collapse of the pore structure. Furthermore, taking into account the different bonding numbers between oxygen and nitrogen,

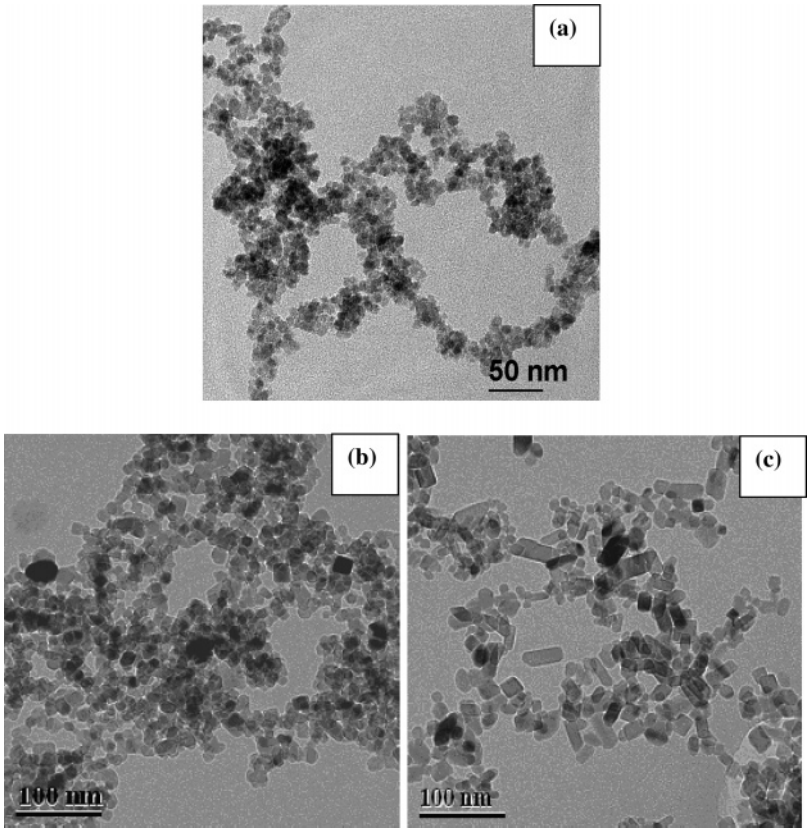

Figure 6. TEM morphologies of (a) TiO_2(DC), (b) TiO_2(SC), and (c) TiO_2N(SC).

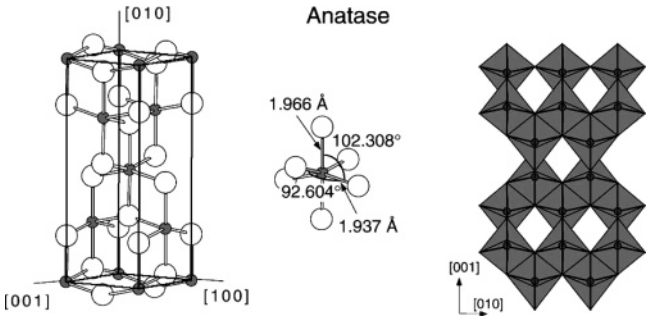

Figure 7. The model of the anatase crystal cell.

TABLE 1: Structural Parameters of Both the Undoped and N-doped TiO2 Samples

sample	$[NH_3]$ (M)	S_{BET}(m^2/g)	V_p (cm^3/g)	d_p (nm)
TiO_2(SC)	0	78	0.42	20
TiO_2N(SC)-1	0.60	90	0.59	17
TiO_2N(SC)-2	1.2	108	0.61	5.0
TiO_2N(SC)-3	2.4	110	0.84	5.2
TiO_2N(SC)-4	3.6	115	0.89	5.1
TiO_2(DC)	0	27	0.037	5.4
P-25	0	45	0.25	20

SCHEME 2: Formation of the Ti_3N Loosen Structure

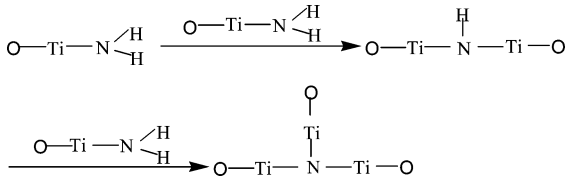

the following structure could be formed when the lattice oxygen was substituted by nitrogen during nitridation of TiO_2(see Scheme 2). This structure seems more loose than the O−Ti−O−Ti−O structure, making the as-prepared sample more porous, corresponding to the larger V_P and thus, the higher S_{BET}.

Figure 8 shows the UV−vis diffuse reflectance spectra of the TiO_2(SC) and TiO_2N(SC) samples. One could see that the undoped TiO_2(SC) could absorb UV light and with a little visible light. Obviously, modification of TiO_2 under SCs resulted in the remarkable shift of absorbance region toward longer wavelength, and even into visible light region, possibly owing to the substitution of the lattice oxygen by nitrogen during the TiO_2 nitridation, which resulted in the narrow band gap by mixing the N_{1S} and the O_{1S} states.[11−13] The light absorbance of the TiO_2N(SC) in the visible light region is of great importance for its practical application since it could be activated even by sunlight.

Figure 9 revealed that the phenol conversion over the TiO_2N(SC)-1 increased almost linearly with the reaction time. On one hand, it suggested that the photocatalytic degradation was zeroth order with the phenol concentration. On the other hand, one can conclude that the phenol degradation proceeded without significant side reactions, which was in accordance with the product analysis by high-performance liquid chromatography (25 cm × 0.46 cm SPHERISORB ODS column, 50% methanol−water mobile phase, UV detector). Only phenol was identified in the reaction solution, showing the complete decomposition of phenol to carbon dioxide under the present conditions.

Figure 10 shows the phenol conversion after reaction for 3 h over different catalysts, from which the following results could be obtained.

1. By examination of the activities of the TiO_2(DC) and TiO_2(SC), it was clear that the treatment under SCs greatly enhanced the activity of the TiO_2 photocatalyst. One possible reason was the higher surface area, larger pore volume, and bigger pore size of the TiO_2(SC), as shown in Table 1, which facilitated the adsorption and diffusion of the phenol molecules. Another important reason was the higher crystallization degree

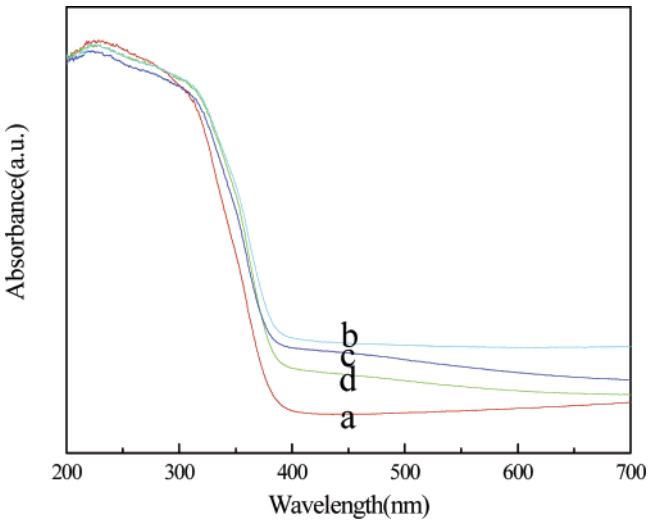

Figure 8. UV−vis diffuse reflectance spectra of (a) TiO_2(SC), (b) TiO_2N(SC)-1, (c) TiO_2N(SC)-2, and (d) TiO_2N(SC)-4.

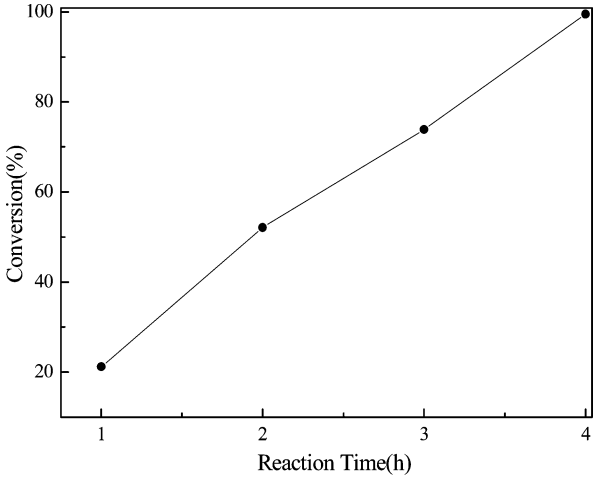

Figure 9. Dependence of phenol conversion on the reaction time over the TiO_2N(SC)-1. Reaction conditions: 0.050 g catalyst, 30 mL 0.05 g/L phenol aqueous solution, three 6-W lamps with characteristic wavelengths of 365 nm as irradiation source mounted at 4 cm above the solution, T = 303 K, stirring rate = 1000 rpm.

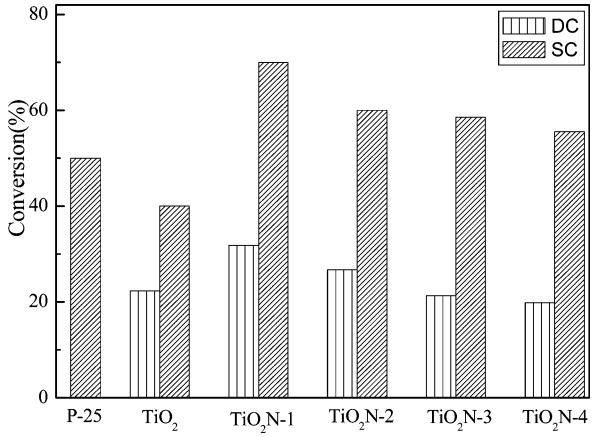

Figure 10. Phenol conversion after reaction for 3 h over different catalysts. Reaction conditions are given in Figure 9.

of anatase phase in the TiO_2(SC), as confirmed by the aforementioned XRD patterns. The well-crystallized anatase could facilitate the transfer of the photoinduced electrons from bulk to surface, which decreased the probability of recombination with photoinduced holes and thus enhanced the quantum efficiency of photocatalysis.[27,28]

2. By comparison of the activities between the undoped TiO_2 and the N-doped TiO_2, one could conclude that the modification of TiO_2 with suitable amount of nitrogen via either DC or SC showed promoting effects on the photocatalytic activity. The maximum activity was observed over the TiO_2N(SC)-1 with the N/Ti molar ratio of 1.73%, which was even more active than the commercially available P-25. The promoting effects of the N modification on the activity could be explained by considering the following factors: (i) The N modification resulted in the higher surface area and larger pore volume, as shown in Table 1. However, this was not convincing because the activity decreased gradually from TiO_2N(SC)-1 to TiO_2N(SC)-4, although the S_{BET} and the V_P still increased. (ii) The N modification resulted in the higher crystallization degree of anatase phase, which was favorable for photocatalysis, as discussed above. (iii) The nitridation resulted in the transfer of the absorbance light toward longer wavelength. As shown in Figure 8, the TiO_2N(SC) exhibited strong absorption in the visible region while the TiO_2(SC) displayed absorption only in UV region. In concern for the wavelength of 365 nm used as irradiation source for the present phenol degradation, the TiO_2N(SC) still exhibited much stronger absorbance than the TiO_2(SC). Thus, the TiO_2N(SC) could be activated more easily than the TiO_2(SC), corresponding to the higher activity. (iv) According to XPS spectra (Figure 1), the N atoms in the nitrides of TiO_2N(SC) samples were electron deficient, which could serve as an electron trap to inhibit the recombination between photoinduced electrons and holes and, thus, promoted the oxidative degradation of phenol.[19] (v) From the FTIR spectra (see Figure 1), the nitridation of TiO_2 under SCs resulted in the formation of surface OH species, which were favorable for the phenol degradation since OH species might serve as the source for producing photoinduced HO• radicals, which acted as a strong oxidizing agent during phenol degradation.[5]

3. The activities of the TiO_2N(SC) samples decreased gradually from TiO_2N(SC)-1 to TiO_2N(SC)-4 obtained in the NH_3/ethanol supercritical fluid with the NH_3 concentration increased from 0.6 to 3.6 M. As mentioned above, the increase of NH_3 concentration had very little influence on the N/Ti molar ratio in the nitrides. But the increase of NH_3 concentration resulted in considerable increase of the surface adsorbed NH_3 molecules. On one hand, very large amount of surface NH_3 molecules was harmful for the activity possibly due to the coverage of too many TiO_2 active sites. On the other hand, the adsorbed NH_3 molecules could serve as Lewis base to capture the photoinduced holes and thus inhibit the oxidative degradation of phenol.[28] The TiO_2N(SC)-1 exhibited the maximum activity, even much higher than the P-25.

4. By consideration that the N-doped TiO_2 catalysts were obtained via different methods, the phenol conversion over the TiO_2N(SC)-1 was 30% higher than the corresponding TiO_2(SC), while the phenol conversion over the TiO_2N(DC)-1 was only 8.5% higher than the corresponding TiO_2(DC). The poor promoting effect of N modification via DC could be understood by considering the absence of nitridation. Thus, only surface NH_3 molecules were present in the TiO_2N(DC) through chemisorption. Although the N modification could also enhance the crystallization degree of anatase phase, which was favorable for the photocatalytic activity, such promoting effect could be diminished by surface adsobed NH_3 molecules, as discussed above.

Conclusions

The above results demonstrated that pretreatment of the TiO_2 precursor in the NH_3/ethanol fluid under SCs was a convenient and powerful way to prepare N-doped TiO_2. The obtained TiO_2N(SC) exhibited very high activity in liquid-phase phenol photodegradation, even higher than commercially available P-25. More specially, the following points are highlighted:

1. The TiO_2(SC) obtained via treatment under SCs exhibited much higher activity than the TiO_2(DC) obtained via DC, which could be mainly attributed to the well-crystallized anatase phase, higher surface area, high surface area, and large pore volume.

2. The N-doped TiO_2 could be prepared by pretreating the precursor in the NH_3/ethanol fluid under SCs. The as-prepared TiO_2N(SC) exhibited much higher activity than the undoped TiO_2(SC). The maximum activity was obtained over the TiO_2N(SC)-1 with the N/Ti molar ratio of 1.73%, which was even much higher than P-25. The promoting effect of N-doping on the activity could be mainly attributed to the increase in crystallization degree of anatase and the formation of both the O−Ti−N and the surface OH species through nitridation, which could extend the light absorbance toward longer wavelength and might supply more HO• radicals for phenol oxidative degradation.

3. The promoting effect of N modification via treatment under SCs was much stronger than that via DCs, since most N dopants were present in the nitrides in the TiO_2N(SC) while the N dopants in the TiO_2N(DC) were present mainly in the form of surface adsorbed NH_3 molecules. These surface NH_3 molecules might cover the active sites and also served as Lewis bases to capture photoinduced holes, which diminished the promoting effect of the N modification. This could also account for the fact that the activity of the TiO_2N(SC) first increased and then decreased with the increase of the N content, since supercritical treatment in ethanol fluid containing very high NH_3 concentration resulted in large amount of surface adsorbed NH_3 molecules which also diminished the promoting effect of the N modification.

Acknowledgment. This work was supported by the National Natural Science Foundation of China (20377031), Shanghai Leading Academic Discipline Project(T0402), and the Natural Science Foundation of Shanghai Science and Technology (02DJ14005, 03DJ14005).

References and Notes

(1) Hoffmann, M. R.; Martin, S. T.; Choi, W.; Bahnemann, D. W. *Chem. Rev.* **1995**, *95*, 69.

(2) Ohtani, B.; Ogawa, Y.; Nishimoto, S. *J. Phys. Chem. B* **1997**, *101*, 3746.

(3) Nazeeruddin, M. K.; Kay, A.; Rodicio, L.; Humphry-Baker, R.; Müler, E.; Liska, P.; Vlachopoulos, N.; Gratzel, M. *J. Am. Chem. Soc.* **1993**, *115*, 6382.

(4) Yamashita, H.; Ichihashi, Y.; Harada, M. *J. Catal.* **1996**, *158*, 97.

(5) Linsebigler, A.; Lu, L. G..; Yates, J. T., Jr. *Chem. Rev.* **1995**, *95*, 735.

(6) Yu, J. C.; Yu, J. G..; Ho, W. K.; Jiang, Z. T.; Zhang, L. Z. *Chem. Mater.* **2002**, *14*, 3808.

(7) Kormann, C.; Bahnemann, D. W.; Hoffmann, M. R. *J. Phys. Chem.* **1988**, *92*, 5196.

(8) Klosek, S.; Raftery, D. *J. Phys. Chem.* **2001**, *105*, 2815.

(9) Qaradawi, Al. S.; Salman, S. R. *J. Photochem. Photobiol. A* **2002**, *48*, 161.

(10) Piera, E.; Ayllon, J. A.; Domenech, X. *J. Peral. Catal. Today* **2002**, *76*, 259.

(11) Sato, S. *Chem. Phys. Lett.* **1986**, *123*, 126.
(12) Irie, H.; Watanabe, Y.; Hashimoto, K. *J. Phys. Chem. B* **2003**, *107*, 5483.
(13) Burda, C.; Lou, Y.; Chen, X.; Chen, X.; Samia, A. C. S.; Stout, J.; Gole, J. L. *Nano Lett.* **2003**, *42*, 403.
(14) Gourinchas-Courtecuisse, V.; Bocquet, F.; Chhor, K.; Pommier, C. *J. Supercrit. Fluids* **1996**, *9*, 222.
(15) Evi, B.; Pegie, C.; Etienne, F. *J. Phys. Chem. B* **2005**, *3*, 31.
(16) Bocquet, J. F.; Chhor, K.; Pommier, C. *Mater. Chem. Phys.* **1999**, *57*, 274.
(17) Grieken, Van. R.; Calleja, G.; Stucky, G. D.; Melero, J. A.; Garcia, A.; Iglesia, J. *J. Langmuir* **2003**, *19*, 3973.
(18) Li, H. X.; Zhu, J.; Li, G. S. *J. Chem. Lett.* **2004**, *33*, 574.
(19) Li, H. X.; Li, G. S.; Zhu, J.; Wan, Y. *J. Mol. Catal.* **2004**, *226*, 93.
(20) Nalo, L. A.; Cerrlos, C. C.; Real, C. *J. Surf. Interface. Anal.* **1996**, *24*, 355.
(21) Shanmugasundaram, S.; Marcin, J.; Horst, K. *J. Phys. Chem. B* **2004**,*108*, 19384.
(22) Kamal, M. S. K.; Mohamed, I. Z. *J. Powder Technol.* **1997**, *92*, 233.
(23) XiaoBo, C.; Clemens, B. *J. Phys. Chem. B* **2004**, *108*, 15446.
(24) Saha, N. C.; Tomkins, H. C. *J. Appl. Phys.* **1992**, *72*, 3072.
(25) Brodsky, C. J.; Ko, E. I. *J. Non-Cryst. Solids* **1995**, *88*, 186.
(26) Harris, M. T.; Brunson, R. R.; Byers, C. H. *J. Non-Cryst. Solids* **1990**, *121*, 397.
(27) Yamazaki, S.; Fujinaga, N.; Araki, K. *J. Appl. Catal. A* **2003**, *210*, 97.
(28) Young, R. A.; Desai, P.; Nauki, A. *J. Mater.* **1989**, *10*, 71.